MULTI-OBJECTIVE OPTIMISATION OF LOW PRESSURE COMPRESSION SYSTEM

Daisuke Sasaki*, Shahrokh Shahpar, Shigeru Obayashi***
***Institute of Fluid Science, Tohoku University, Sendai, Japan**
****Aerothermal Methods, Rolls-Royce plc, Derby, UK**

Keywords: *Aerodynamic Optimisation, Multi-Objective Optimisation, Evolutionary Algorithms, Computational Fluid Dynamics, LPC System*

Abstract

Adaptive Range Multi-Objective Genetic Algorithm (ARMOGA) has been developed to obtain trade-offs more efficiently than conventional Multi-Objective Evolutionary Algorithms. In this paper, the performance of ARMOGA is demonstrated through a multi-objective design optimisation of Bypass Fan Outlet Guide Vanes as part of the Low Pressure Compression (LPC) system. In the present optimisation, the objectives of the LPC system are to reduce the circumferential pressure variation at the inlet boundary and mixed-out total pressure loss at selected radial height. These objective functions are evaluated by an in-house, parallel, high-fidelity CFD solver. Throughout the optimisation, ARMOGA has shown reasonable performance for obtaining trade-offs even with a small number of evaluations.

1 Introduction

Industrial problems often have many design objectives, which may be conflicting with one another. Hence, trade-off studies may be required. To identify global tradeoffs, the problem can be treated as Multi-Objective (MO) optimisation. MO optimisation seeks to optimise components of a vector-valued objective function. In general, the solution to this problem is not a single point like single-objective optimisation, but a family of points known as the Pareto-optimal set. Pareto solutions, which are members of the Pareto-optimal set, represent trade-offs among multiple objectives. Conventionally, gradient-based methods have been used for MO problems. However, gradient-based methods are not efficient to obtain trade-offs because weights between objectives and initial starting points have to be changed to obtain different Pareto solutions, they are not known *at priori*.

Nowadays, MOEAs (Multi-Objective Evolutionary Algorithms) have gained popularity because of its efficient and effective search for obtaining Pareto solutions [1]. As it is well-known, EAs (Evolutionary Algorithms) tend to require a large number of evaluations. This could be a major inhibitor in using MOEAs for aerodynamic optimisation using time-consuming high-fidelity Computational Fluid Dynamics (CFD). The latter is required to obtain accurate aerodynamic performance. Hence, a real-coded Adaptive Range Multi-Objective Genetic Algorithm (ARMOGA) has been developed for the reduction of number of evaluations to make it practical to apply ARMOGA to aerodynamic optimisation problems [2].

The aim of this research is to demonstrate a multi-objective design optimisation of Bypass Fan Outlet Guide Vanes (OGVs) as part of the Low Pressure Compression (LPC) system as shown in Fig.1 In this study, an in-house, parallel, high-fidelity CFD solver is used to compute the flow solutions for this system.

2 Evolutionary Algorithm

EA is a generic term of population-based stochastic optimisation methods such as Genetic Algorithm (GA), Evolutionary Strategy (ES)

and Evolutionary Programming (EP). GAs simulate the mechanism of the natural evolution, where a biological population evolves over generations to adapt to an environment by selection, crossover and mutation, as shown in Fig.2. Fitness, the individual, and genes in the evolutionary theory correspond to the objective function, design candidate, and design variables in design optimisation problems, respectively.

GAs search from multiple points in the design space simultaneously and stochastically, instead of moving from a single point deterministically like gradient-based methods. This feature prevents design candidates from trapped in local optimum. Moreover, GAs do not require computing gradients of the objective function. These characteristics lead to following advantages of GAs: 1, GAs have capability of finding global optimal solutions. 2, GAs can be processed in parallel efficiently. 3, high fidelity CFD codes can easily be adapted to GAs without any modification. 4, GAs are not sensitive to any noise that might be presented in the results. 5, GAs are less prone to premature failure.

2.1 Multi-Objective Evolutionary Algorithm

To identify trade-offs among several objective functions, MO optimisation has to be conducted. Unlike single-objective optimisation, the fitness of each design candidate is assigned based on the Pareto-optimality. The rank of a design is given by the number of solutions which dominate the design as shown in Fig.3. The aim of MO optimisation is to seek solutions which are assigned rank 1. In ARMOGA, Fonseca and Fleming's Pareto ranking method is used [3].

2.2 Adaptive Range Multi-Objective Genetic Algorithm

To reduce the large computational burden, the reduction of the total number of evaluations is needed. Adaptive Range Genetic Algorithm (ARGA), which originally proposed by Arakawa and Hagiwara [4], then extended by Oyama et al [5], is a quite unique approach to solve such problems efficiently.

ARMOGA has been developed based on the real-coded ARGA to deal with multiple Pareto solutions for the multi-objective optimisation. The main difference between ARMOGA and a conventional MOEA is the introduction of the range adaptation. The flowchart of ARMOGA is shown in Fig.4. Population is reinitialised at every M generations for the range adaptation so that the population advances toward promising regions.

The basis of ARMOGA is the same as ARGA, but a straightforward extension may cause a problem in the diversity of the population. To better preserve the diversity of solution candidates, the normal distribution for encoding is changed. Figure 5 shows the search range with the distribution of the probability. Plateau regions are defined by the design ranges of chosen solutions. Then the Normal distribution is considered at the both sides of the plateau.

ARMOGA is able to find Pareto solutions more efficiently than conventional EAs because of the concentrated search of the promising design space out of the large, initial design space. ARMOGA can adapt its search region as shown in Fig.5. In contrast, conventional EAs' search region remains unchanged. Re-initialisation helps to maintain the population diversity.

3 Single-Height Optimisation of LPC System

In the present optimisation, an in-house, parallel, Navier-Stokes solver [6-10] is used to evaluate the flow at LPC system to reduce the large computational burden. Figure 6 shows a 2-D slice through OGV-Pylon-RDF (Radial Drive Fairing) Bypass Duct system of a modern jet engine considered in the study. The OGV ring consists of 52 blades that has a big influence on the performance of the system. The objective of the present research is to demonstrate efficient calculation of Pareto fronts to extract information to reduce the circumferential pressure variation at the inlet boundary and mixed-out total pressure loss calculated between

inlet boundary and rear of OGVs as shown in Fig.6.

3.1 Optimisation Definition

The objectives of the optimisation is to minimise the mixed-out total pressure loss and to minimise the root mean square of circumferential pressure variation at inlet as described below.
LOSS:

$$Min.\ Loss(\%) = \frac{P_{total}^{in} - P_{total}^{out}}{P_{total}^{in} - P_{static}^{in}} \times 100 . \qquad (1)$$

RMSPV:

$$Min.\ \sqrt{\frac{\sum_{i=1}^{N}(p_i - \bar{p})^2}{N}}, \qquad (2)$$

$$\text{where } \bar{p} = \frac{\sum_{i=1}^{N} p_i}{N}.$$

The design parameters conducted in the study consists of the re-staggering of sections of the 52 OGVs. To reduce the number of design variables, the geometric patterns of OGVs' stagger angle are represented based on the Fourier series (Fig.7) as follows:

$$Var_i = A_0 + \sum_{j=1}^{N}\left[A_j \sin\left((i-1)\frac{2\pi}{N_{OGV}}\right)\right] + \sum_{j=1}^{N}\left[B_j \cos\left((i-1)\frac{2\pi}{N_{OGV}}\right)\right] \qquad (3)$$

$$Var_i = \frac{Var_i}{\max\left|Var_i\right|_{i=1,N}} \times AMPL . \qquad (4)$$

where N: Number of harmonics,
N_{OGV}: Number of OGVs,
i: ith OGV.

The fifty-two design parameters, *i.e.* VAR_i, are defined by 15 design variables (N=7), namely Fourier coefficients A_j and B_j. Each value of the pattern is then divided by the maximum and multiplied by an amplitude to maintain a maximum practical variation of the design variables. In this optimisation, the amplitude (*AMP*L) is set to eight degrees. The new geometric patterns are added to the base geometry that has a uniform distribution of OGVs. Figure 8 shows an example of the geometric patterns of 52 OGVs' re-stagger angle.

3.2 Optimisation Results

The present optimisation was conducted using nearly 500 CFD runs (12 individuals for 40 generations). Each CFD evaluation takes about 25 minutes using eight CPUs (Pentium3-450MHz). To reduce the computational time, all CFD computations start from a fully converged solution of the base geometry. Figure 9 shows a sample of optimisation results. In the figure, non-dominated solutions obtained at the initial, 20 and 40 generations are shown. It represents the overview of the evolution of the design. Objective-function values in the figure are normalised by the base geometry as follows:

$$\Delta(\%) = \frac{Value_{Base\ Geometry} - Value_{Design}}{Value_{Base\ Geometry}} \times 100 . \qquad (5)$$

Totally, 11 non-dominated solutions are finally obtained and it shows the trade-offs between the pressure variation and the total pressure loss. Final non-dominated solutions having minimum pressure variation (MIN_RMSPV) and total loss (MIN_LOSS) are chosen to compare the flow field in Fig.10. The flow field of MIN_LOSS seems to be smooth. Instead, MIN_RMSPV has thick wake regions and it causes the rise of total pressure loss. ARMOGA can obtain 62% reduction of pressure variation compared to the base geometry. On the other hand, all the designs have worse total pressure loss values. At mid-height, it is difficult to reduce the total loss with the current design space and partly because OGVs could have a maximum stagger angle of eight degrees.

4 Multi-Height Optimisation of LPC System

In the previous section, single-height optimisation was performed. To consider a more

realistic design, multi-height optimisation is conducted here. In addition to 50%, 10% and 90% heights of LPC system is assumed to demonstrate the multi-objective optimisation of LPC system as shown in Fig.11.

4.1 Optimisation Definition

The objectives of the present optimisation is the same as previous, but there are six objectives to be minimised because three height is considered. It may cause the large increase of computational time, because EA generally requires more evaluations if the number of objective function increases. To prevent the large amount of computations, six objective functions are combined to form the new two objectives: the average of total pressure losses in Eq.(1) and the average of pressure variation in Eq.(2) at three heights.

Average LOSS:

$$Min.\ \ \frac{1}{3}LOSS(10\%)+\frac{1}{3}LOSS(50\%)+\frac{1}{3}LOSS(90\%)\cdot \qquad (6)$$

Average RMSPV:

$$Min.\ \ \frac{1}{3}RMSPV(10\%)+\frac{1}{3}RMSPV(50\%)+\frac{1}{3}RMSPV(90\%)\cdot \qquad (7)$$

In the main routine of the ARMOGA, above two objective-function values are used to select parents to generate new offspring. Six objectives are directly considered to form the new search range of each design variable to keep the search region where six-objective non-dominated solutions exist.

Re-staggering angles of the 52 OGVs at three heights has to be defined in an efficient manner to control the number of design variables. The patterns of OGVs' stagger angle are represented by the Fourier series and three zero harmonics are introduced to change the base angles of each OGV's pattern as shown in Fig.12.

$$Var_i^{height} = A_0^{height} + Var_i \qquad (8)$$

where A_0^{height}: Zero harmonics at three heights (10, 50, 90%).

The OGVs' re-stagger patterns are represented by 17 variables (N=7 and three zero harmonics). Table 2 describes the upper and lower boundaries of the design variables. Unlike the previous optimisation, maximum amplitude ($AMPL$) is not used to provide more freedom to the geometric patterns of OGVs. However, it is possible that the geometry has impractically large angles. To prevent this problem, the amplitude of each design must be lower than four degrees.

ARMOGA is used to solve the optimisation problem having six objective functions, 17 design variables and a constraint. Selection for crossover and mutation is based on the Pareto ranking method (Fig.3) coupled with Best-N selection considering two objectives of the average. Instead, six objectives are directly used to evaluate the solutions to sample the better solutions for the range adaptation. The range adaptation starts at 5th generation and it is occurred every 5 generations. To prevent computing time being wasted to search infeasible solutions, new design candidates are generated again and again until they satisfy the constraint.

4.2 Optimization Results

Population size and number of generation are set to 12 and 20, respectively to solve the present optimisation problem by ARMOGA. Each individual requires 1.5 hours for the evaluation because each CFD evaluation takes about 30 minutes using eight CPUs (Pentium3-450MHz). To reduce the computational time, all CFD starts from a fully converged solution of the base geometry at each height.

As a result of the optimisation including nearly 700 CFD runs, five non-dominated solutions were obtained in objective-function space of averaged total loss and pressure variation as shown in Fig.13. In the figure, final

non-dominated front progressed largely compared to initial front in averaged space. As the original optimisation has six objective functions, all solutions are sampled to form non-dominated solutions in the six objective-function space. In total, 21 non-dominated solutions are obtained in the six objective-function space. It is not easy to understand the trade-off represented by 21 non-dominated solutions because these solutions form the trade-off in the six objective-function space. Therefore, all non-dominated solutions are projected onto the two-dimensional surface between pressure variation and total pressure loss at each height in Fig.14. The figures indicates the trade-off between pressure variation and total loss at each height. Three solutions (A, B, C) are chosen to realise the trade-off at 10% height. Solution A has lower pressure variation and higher loss, B has lower pressure variation and lower loss and C has higher pressure variation and lower loss. Designers can choose the design from the trade-off according to their requirements.

To understand the present design problems, six objective-function values of three heights are projected onto the same normalised axes of pressure variation and loss in Fig.15. Three trade-offs between pressure variation and loss (I, II, III) are represented in the figure. Non-dominated fronts I, II and III represent the trade-off at 10, 50 and 90% heights, respectively. At 10 and 50% heights, it is easy to reduce the pressure variation while maintaining the loss. On the other hand, front III indicates that it is impossible to reduce the pressure variation and the loss at 90% height simultaneously. In Fig.16, Mach contours of solutions D (minimum RMSPV at 90%) and E (minimum LOSS at 90%) are shown. Solution E has low total pressure loss, but the flow flied shows still many thick wake regions. Since the distance between row of OGVs and Pylon or RDF is near, it is not easy to reduce the loss by changing re-stagger angles of OGVs. Other design parameters will be required to reduce the pressure variation while maintaining the loss at 90% height.

Another visualisation technique is also applied to study the present trade-offs. Self-Organising Map (SOM, [11]) is a visualisation tool that can produce a topology preserving map from high dimensional data, thus it can be used as a cluster analysing tool. As there are many objective functions in the current optimisation problem, the cluster analysis of the six objective functions are conducted to identify design trade-offs. The resulting non-dominated fronts are projected onto a two-dimensional map. Figure 17 shows the resulting SOM with seven clusters. For a better understanding, positions of non-dominated solutions that minimise each objective function are also described. The design Min.LOSS(90%) locates the upper right corner, on the contrary, the design Min.RMSPV(90%) locates the opposite position. In the lower right corner, the designs to reduce both the loss and the pressure variation are located. Figure 18 shows the same SOM contoured by six design-objective values, which are standardised based on the base geometry by dividing the maximum or minimum value of each design-objective function. From the figure, SOMs coloured by pressure variations at 10 and 50% show similar pattern, their lower values are distributed at the upper left corner. Their patterns are roughly opposite of the loss at 90%. It is also quite apparent that the colour pattern of the loss at 90% is quite the opposite to that of the pressure at 90%.

The following trade-off information is assumed by summarising the above discussion. It is easy to reduce the pressure variations of the three heights at the same time. The pressure variation can be reduced while maintaining the loss at 10% and 50%, but not at 90%. To find a reasonable way to reduce the loss at 90% without any increase in the pressure variation is the key point for the present optimisation. Indeed, the loss at 90% is distributed in a wide range visualised by the trade-off graph as shown in Fig. 19. It also reveals that the loss at 10% is another important factor because there are two groups categorised by better and worse values compared to the base geometry. In an actual design, designers can choose the desirable

design from the trade-off graph based on their requirements.

Finally, a solution F is chosen to compare the base geometry. It has lower values of all six objective functions compared to the base geometry in Table 3. Figure 20 shows the circumferential pressure variation at inlet of the design F and the base geometry. Large reduction of pressure variation can be seen at 10% height. Pressures near the pylon consistently decrease at all heights to reduce the pressure variation at inlet. Indeed, the distribution of OGVs' re-stagger angle shows that it tries to reduce the pressure near the pylon in Fig.21.

5 Conclusion

To evaluate the performance of ARMOGA, MO optimisation was performed for OGV-Pylon-Bypass Duct system. In total of 500 CFD evaluations were conducted and 11 non-dominated solutions were obtained in single-height optimisation. The Pareto front represents the trade-offs between the pressure variation at the inlet boundary and mixed-out total pressure loss.

Multi-height optimisation was then performed to consider more practical problems. Six-objective optimisation problem was efficiently solved by ARMOGA and 21 non-dominated solutions were obtained in six objective-function space by nearly 700 CFD runs. Trade-off analysis reveals that it is easy to reduce the pressure variation while maintaining the loss at 10 and 50%, and it is difficult to do that at 90% by just changing the re-stagger angles. The design that is superior to the base geometry in all six design objectives has the geometric patterns of OGVs to reduce the pressure near the pylon for all three heights.

The Pareto front provides valuable information to designers to carry out trade-off studies. In addition, ARMOGA can obtain those trade-offs efficiently. Therefore, ARMOGA has proved to be a good optimisation tool for turbomachinery aerodynamic design problems requiring large evaluation time of CFD.

Acknowledgement

This research has been performed during the first author's stay at Rolls-Royce plc under industrial trainee program.

References

[1] Deb, K. *Multi-objective optimization using Evolutionary Algorithms*. John Wiley & Sons, Ltd., Chichester, 2001.

[2] Sasaki, D., Obayashi, S. and Nakahashi, K. Navier-Stokes optimization of supersonic wings with four objectives using Evolutionary Algorithm. *Journal of Aircraft*, vol. 39, No. 4, pp 621-629, 2002.

[3] Fonseca, C. M. and Fleming, P. J. Genetic Algorithms for Multiobjective Optimization: Formulation, Discussion and Generalization. *Proc of the Fifth International Conference on Genetic Algorithms*, San Mateo, pp 416-423, 1993.

[4] Arakawa, M. and Hagiwara, I. Development of Adaptive Real Range (ARRange) Genetic Algorithms. *JSME International Journal*, Series C, Vol. 41, No. 4, pp 969-977, 1998.

[5] Oyama, A., Obayashi, S. and Nakamura, T. Real-coded Adaptive Range Genetic Algorithm applied to transonic wing optimization. *Applied Soft Computing*, Vol. 1, No. 3, pp 179-187, 2001.

[6] Shahpar, S., Giacche, D. and Lapworth, L. Multi-Objective Design and Optimisation of Bypass Outlet-Guide Vanes. ASME Paper GT-2003-38700, June 2003.

[7] Shahpar, S., and Lapworth, L., "PADRAM: Parametric Design and Rapid Meshing System for Turbomachinery Optimisation," ASME Paper GT-2003-38698, June 2003.

[8] Muller, J.-D., and Giles, M. B., "Edge-Based Multigrid Schemes for Hybrid Grids," Proceedings of the Sixth ICFD Conference on Numerical Methods for Fluid Dynamics, Oxford, 1998.

[9] Moinier, P., and Giles, M. B., "Preconditioned Euler and Navier-Stokes Calculations on Unstructured Grid," Proceedings of the Sixth ICFD Conference on Numerical Methods for Fluid Dynamics, Oxford, 1998.

[10] Spalart, P. R., and Allmaras, S. R., "A One-Equation Turbulence Model for Aerodynamic Flow," AIAA 92-0439, 1992.

[11] Kohonen, T. *Self-Organizing Maps*. Springer, Berlin, 1995.

Table 1 Upper and lower boundaries of design variables

	A_0	$A_{1,..,7}$	$B_{1,..,7}$
Upper Boundary	3.0	2.0	2.0
Lower Boundary	-3.0	-2.0	-2.0

Table 2 Upper and lower boundaries of design variables

	A_{01} (10%)	A_{02} (50%)	A_{03} (90%)	$A_{1,..,7}$	$B_{1,..,7}$
Upper Boundary	1.0	1.0	3.0	2.0	2.0
Lower Boundary	-8.0	-8.0	-3.0	-2.0	-2.0

Table 3 Objective-function values of solution F

	10%	50%	90%
RMSPV	-53.1	-42.4	-22.5
LOSS	-25.7	-10.0	-11.5

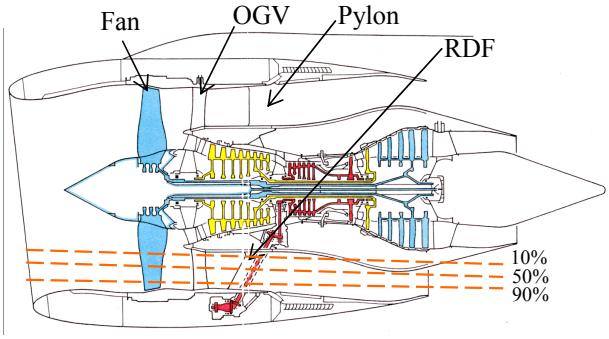

Fig. 1. Low Pressure Compression System.

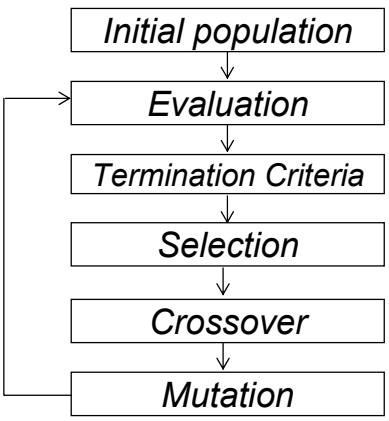

Fig. 2. Flowchart of GAs.

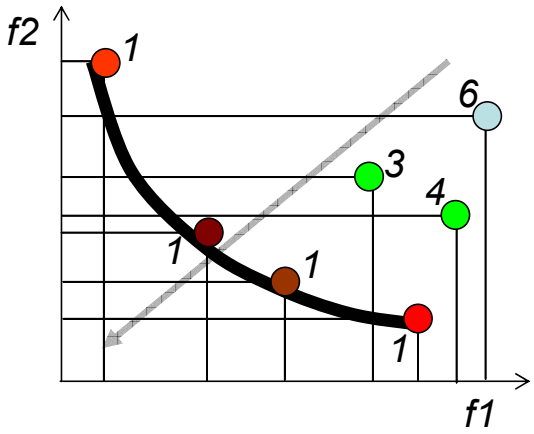

Fig. 3. Pareto Ranking Method.

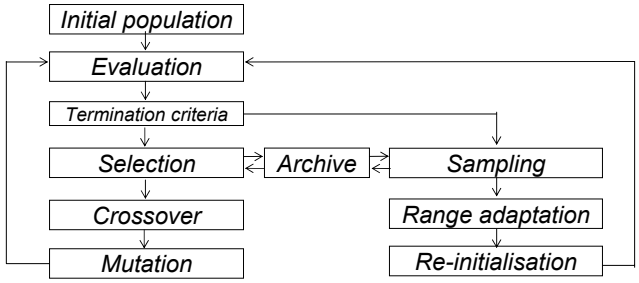

Fig. 4. Flowchart of ARMOGA.

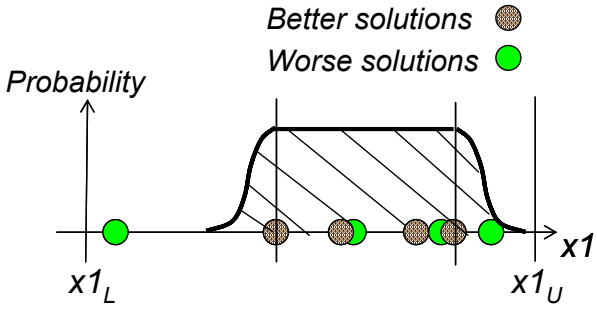

Fig. 5. Sketch of Range Adaptation.

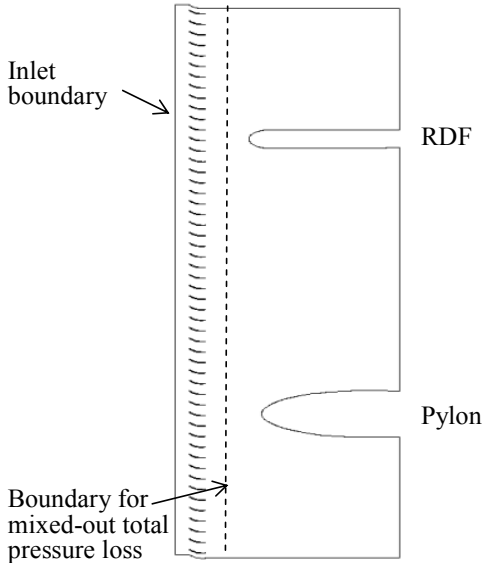

Fig. 6. Axial Locations of OGV-Pylon-RDF System.

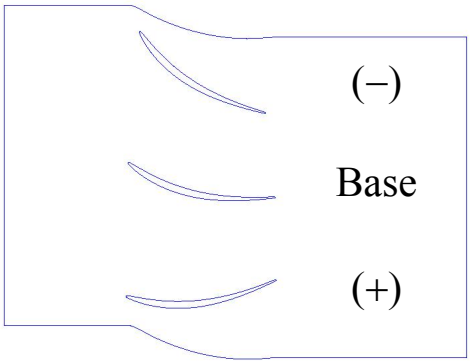

Fig. 7. Re-Stagger of Sections.

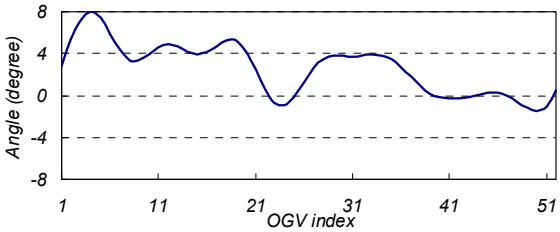

Fig. 8. Geometric Patterns of 52 OGVs' Re-Stagger Angle.

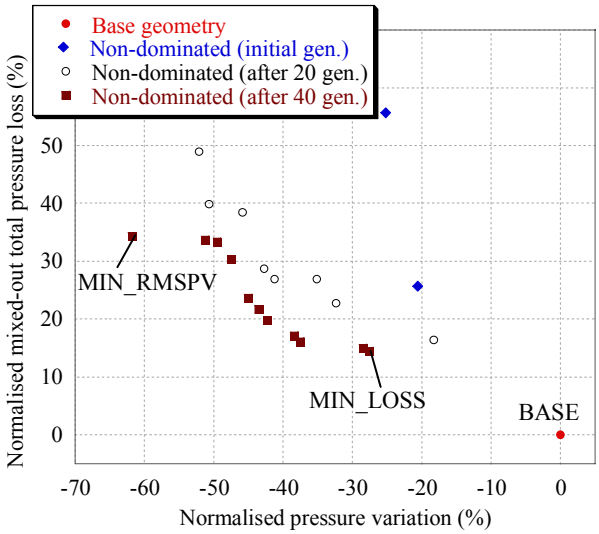

Fig. 9. Non-Dominated Solutions and the Base Geometry in Normalised Objective-Function Space.

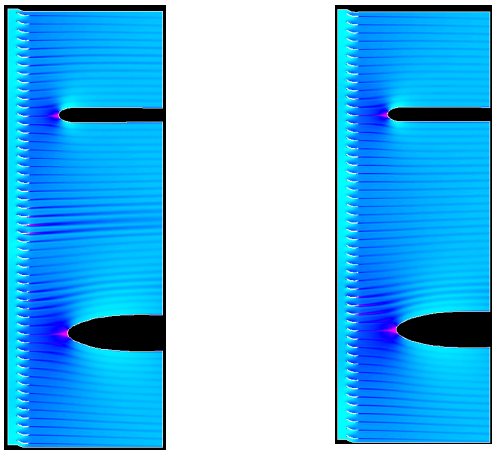

(a) MIN_RMSPV (b) MIN_LOSS

Fig. 10. Mach Contours of Non-Dominated Solutions.

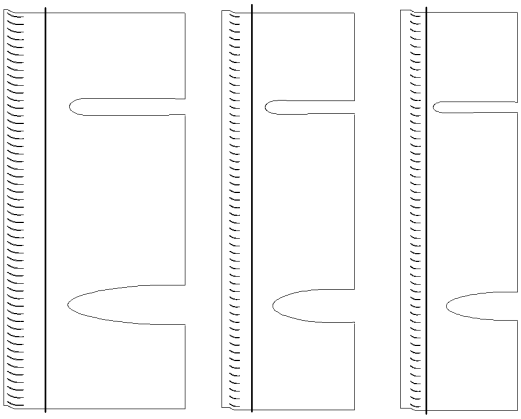

(a) 10% (b) 50% (c) 90%

Fig. 11. Axial Locations of OGV-Pylon-RDF System at Three Heights.

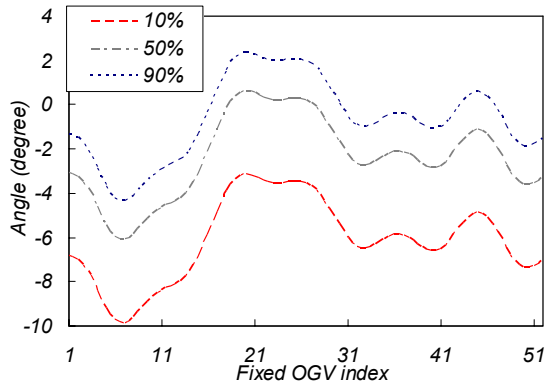

Fig. 12. Geometric Patterns of 52 OGVs' Re-Stagger Angle at Three Heights (10, 50 and 90%).

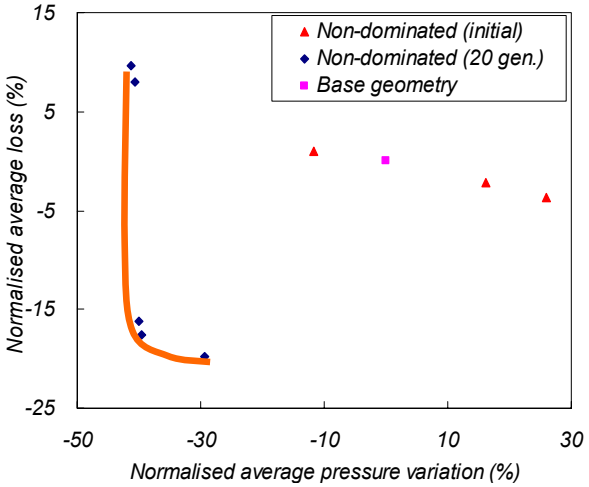

Fig. 13. Non-Dominated Solutions at Initial and 20th Generations and Base Geometry in Averaged Objective-Function Space.

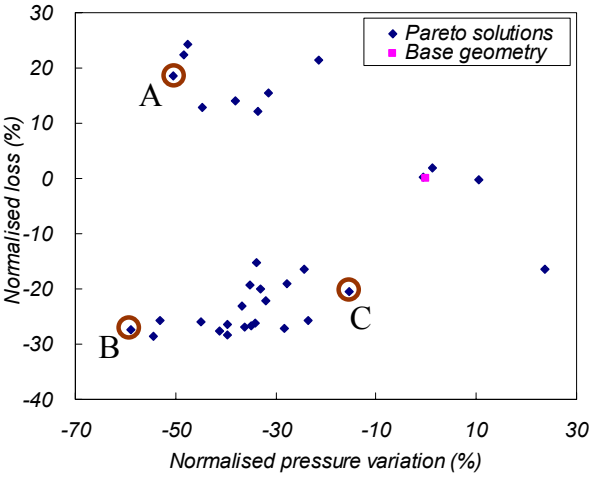

(a) 10%

Fig. 14. Non-Dominated Solutions Considering Six Objectives in Objective-Function Space of Pressure Variation and Loss. (Cont'd)

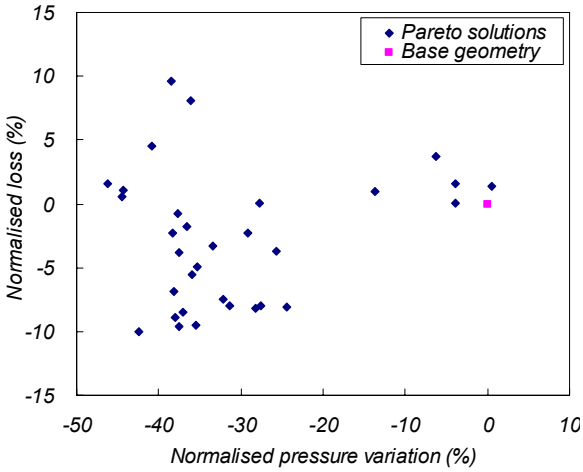

(b) 50%

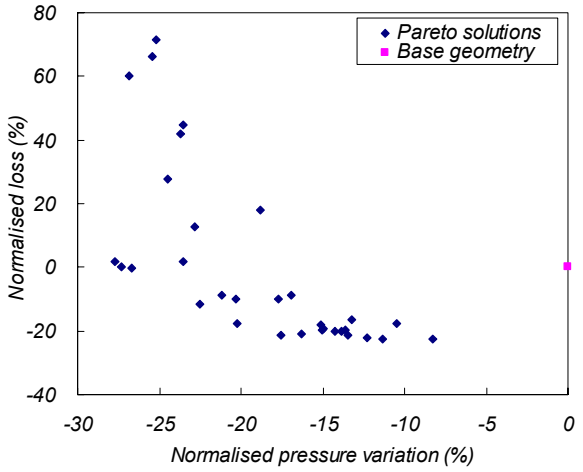

(c) 90%

Fig. 14. Non-Dominated Solutions Considering Six Objectives in Objective-Function Space of Pressure Variation and Loss.

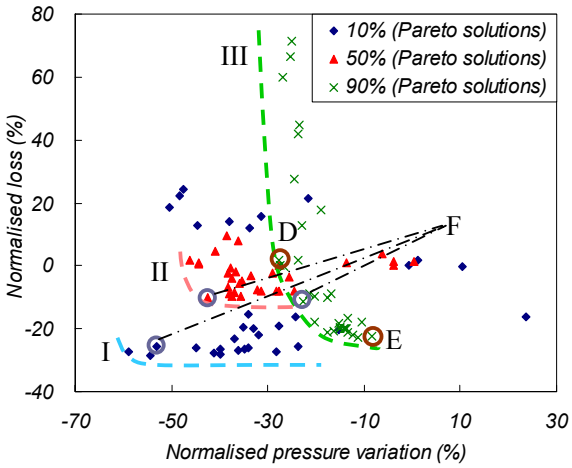

Fig. 15. Non-Dominated Solutions Projected onto the Same Axes Between Pressure Variation and Loss.

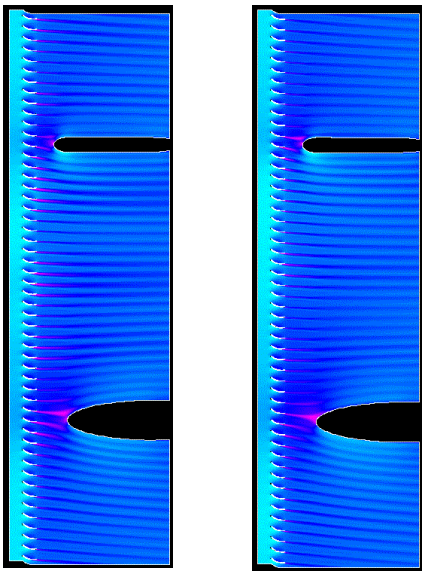

(a) Solution D (b) Solution E

Fig. 16. Mach Contours at 90% Height of Solutions D and E.

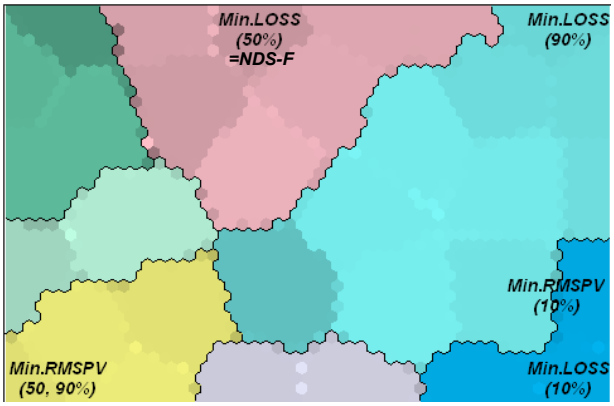

Fig.17. SOM of Six Objective-Function Values.

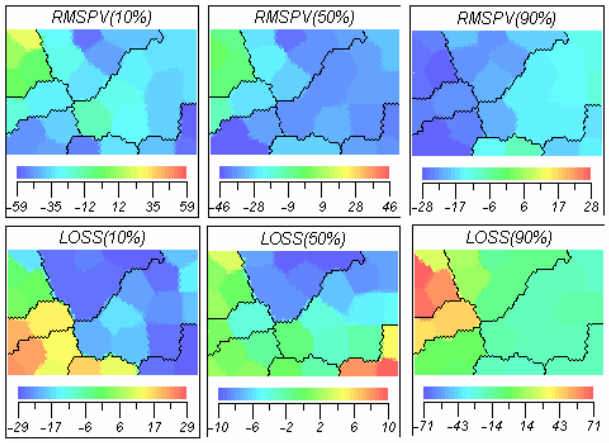

Fig. 18. SOM Contoured by Each Standardised Design Objective.

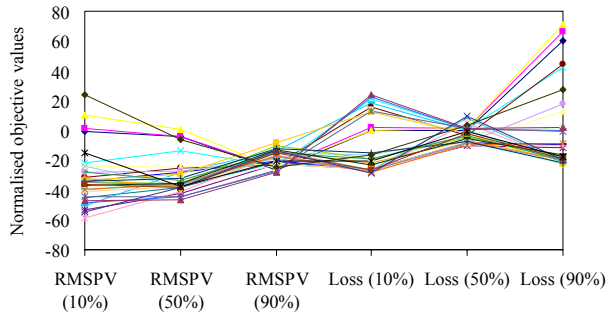

Fig. 19. Trade-Off Graph For Six Objectives.

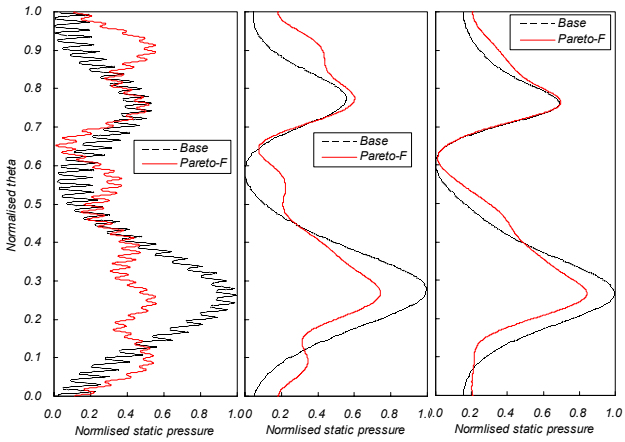

(a) 10% (b) 50% (c) 90%

Fig. 20. Circumferential Pressure Variations of Non-Dominated Solution F and Base Geometry.

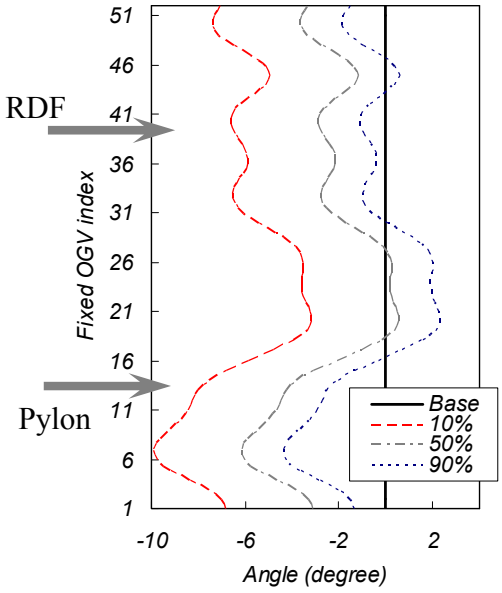

Fig. 21. Geometric Patterns of OGVs' Re-Stagger Angles of Solution F.